Comparison of hyperspherical versus common-reaction-coordinate close-coupling methods for ion-atom collisions at low energies

Anh-Thu Le,[1,*] C. D. Lin,[1] L. F. Errea,[2] L. Méndez,[2] A. Riera,[2] and B. Pons[3]
[1]*Department of Physics, Cardwell Hall, Kansas State University, Manhattan, Kansas 66506, USA*
[2]*Laboratorio Asociado al CIEMAT de Física Atómica y Molecular en Plasmas de Fusión, Departamento de Química Universidad Autónoma de Madrid, 28048 Madrid, Spain*
[3]*Centre Lasers Intenses et Applications (UMR CNRS), Université de Bordeaux I, 351 Cours de Libération, 33405 Talence Cedex, France*
(Received 22 December 2003; published 3 June 2004)

We present detailed comparisons between the two quantal approaches—hyperspherical close-coupling and common-reaction-coordinate close-coupling methods—on an exemplary case of $He^{2+}+H(1s)$ collisions at center-of-mass energy from 20 eV up to 1.6 keV. It is shown that the partial-wave charge-transfer cross sections from the two approaches agree very well at low energy below 200 eV down to 30 eV. This good agreement is a strong indication of the validity of both methods. The small difference at very low energies and the convergence with respect to the number of channels in both approaches at higher energies are also discussed.

DOI: 10.1103/PhysRevA.69.062703 PACS number(s): 34.70.+e, 34.10.+x, 31.15.Ja

I. INTRODUCTION

Inelastic and charge-transfer reactions between atoms or ions at low energies govern the behavior of gaseous media. This concerns a wide range of questions of practical importance from laboratory to terrestrial and astrophysical environments. Over the past few decades, different theoretical methods have been used to evaluate the reaction cross sections that are required for a quantitative understanding of these media [1]. For slow collisions the electron is moving in the field of two slowly moving nuclei such that the collision complex can be approximated as a transient molecule. Therefore, molecular orbitals (MO's) are the natural representation for describing slow ion-atom or atom-atom collisions. This forms the basis of the well-known perturbed-stationary-state (PSS) approximation, introduced by Massey and Smith [2] more than half a century ago. In the PSS approximation, the total wave function is expanded in terms of molecular orbitals, similar to the adiabatic Born-Oppenheimer (BO) approximation for molecules where the internuclear separation is an adiabatic parameter.

In the PSS approach, the numerical calculation of cross sections usually proceeds in two steps: the quantum chemical treatment of the transient molecule and the subsequent treatment of the heavy particles dynamics. However, ever since its introduction, this intuitively attractive PSS model is known to have many defects because the molecular orbitals in the BO approximation do not satisfy correct asymptotic scattering boundary conditions. These defects are well documented, including incorrect dissociation thresholds, nonvanishing asymptotic couplings, and the calculated cross sections not Galilean invariant. Although the defects are well known, the remedies are less obvious. Despite these difficulties, cross sections and rate constants for many different colliding systems have been calculated in response to the need in applications.

For high-energy collisions where the motion of the nuclei may be treated classically, the remedy is centered on the inclusion of "electron translation factors" (ETF's) in the expansion of the electronic wave function [3]. The ETF, noncontroversial in separated-atom bases, has, however, continued to trouble treatment with molecular orbitals. The difficulties arise from the conceptual incompatibility of the translational factors, which associate each electron with a specific fragment, and the BO molecular basis in which each electron moves in a fixed-nuclei complex. Nevertheless, the introduction of ETF's removes the major defects of the standard PSS approximation and excellent agreement with experiments have been obtained from such calculations [1,4,5]. Although the form of the ETF is well established for atomic bases, there are several choices for molecular bases. The generally accepted solution, for collision energies where ionization processes are not significant, is the use of a common translation factor [6], where all the molecular functions are multiplied by the same ETF, which is expressed in terms of a switching function that allows one to fulfill the initial condition; this switching function usually contains adjustable parameters, which is sometimes taken as a drawback of the method, but an optimized ETF improves the convergence speed of the expansion [7]. There is another different approach—the advanced adiabatic approximation [8], which expands the electronic wave function onto dynamically scaled molecular states and employs the theory of hidden crossings (HC's) [9] to describe the inelastic transitions. In this approach a generalized (common) ETF is also introduced to fulfill the correct boundary conditions.

For low-energy collisions where the motion of the nuclei is treated quantum mechanically, the concept of electron translational factors loses its meaning. Despite this fact, similar ETF-modified molecular orbitals have been used in the quantum approach [10,11]. In the meanwhile, the so-

*Electronic address: atle@phys.ksu.edu

called common reaction coordinates (CRC's) have been introduced since late 1960s [12–14] and implemented since the late 1980s and 1990s to obtain cross sections for a few collision systems at low energies [15–17]. Criteria for choosing the reaction coordinates have been proposed and used in the calculations [18,19], but similar to the ETF's, their choices are not unique. Although the CRC method has been tested by experimental data at high energies, the results obtained from this method have not been adequately tested at low energies, especially since high-quality experimental data are hard to come by for low-energy ion-atom collisions. While the experimental situations have been improved to some extent from merged beam experiments in simple ion-atom collision systems in the past decade [20], such measurements can still only give total electron capture cross sections and thus the reliability of the CRC method has not yet been critically tested, especially for the weak channels.

Within the last year, a new implementation to low-energy ion-atom collisions based on the hyperspherical close-coupling (HSCC) method has been developed. The hyperspherical method has been widely used in a variety of three-body systems [21], from reactive atom-diatom [22,23], electron-atom [24,25], and positron-atom [26,27] collisions to three-body recombinations [28]. The HSCC method has been employed to obtain charge-transfer and excitation cross sections for a number of simple ion-atom collision systems so far [29–33] with results in general agreement with experiments when available. In two cases, one in proton-Na [30] and the other in $Be^{4+}+H$ and $Si^{4+}+H$ [31], the total charge transfer cross sections from the HSCC method have been shown to agree rather well with the previously published CRC results, except for small differences at very low energies (of the order of a few eV or less). Such a comparison is interesting since the good agreement establishes the validity of both the HSCC and CRC methods. Furthermore, it confirms that the CRC method can be used to obtain reliable inelastic or charge-transfer cross sections at low energies despite the parameters introduced in the choice of reaction coordinates. This is of practical importance since the HSCC method can be employed only for a one-electron ion-atom collision systems while the CRC method has been applied to few-electron ion-atom collisions [34,35].

The goal of the present paper is to further test the agreement between the HSCC and CRC methods, at the partial-wave cross section levels and over a broad range of collision energies. For this purpose we used the HSCC and CRC methods to calculate charge-transfer cross sections in $He^{2+}+H(1s)$ collisions for energies from 20 eV up to 1.6 keV.

This system has been analyzed for different ranges of energy by many authors using different versions of PSS as well as HC theory [36–42]. It should be noted, however, that there exist few quantal approaches for $He^{2+}+H$ collisions at low energies. The first quantal close-coupling calculations were reported by van Hemert *et al.* [10], who used semiclassical ETF's but solved the motion of the heavy particles quantum mechanically. An alternative approach is the work by Fukuda and Ishihara who used the distorted atomic orbital (DAO) approach [43]. Quite recently, Liu *et al.* [29] performed HSCC calculations for this system using four adiabatic channels. In this paper HSCC and CRC calculations were performed by each one of our groups separately such that we can compare the cross sections at the partial-wave levels, as well as the coupling matrix elements. This would help to establish that the two approaches indeed agree even at the differential level.

This paper is organized as follows. In Sec. II we first summarize the HSCC and CRC methods briefly. The approximations used in each method will be stressed. It will be shown that the hyperspherical radius which is the adiabatic parameter in the HSCC method is very similar to the reaction coordinate ξ used in the CRC method. This allows us to even compare the potential curves and the coupling terms directly. In Sec. III, we present detailed comparisons of the results from the HSCC and CRC methods, on the level of nonadiabatic couplings and partial-wave capture cross sections. The last section gives a summary and conclusions. All the energies are given in the center-of-mass frame. Atomic units are used unless otherwise indicated.

II. THEORY

A. Hyperspherical close-coupling method

The details of the HSCC theory are given in Liu *et al.* [29]. In this subsection we describe the basic ingredients of the method. We also give here a description of a modification of the method—namely, the diabatization procedure used to adequately compare with the results from CRC. In the center-of-mass frame we solve the time-independent Schrödinger equation for the three-body HeH^{2+} system in the mass-weighted hyperspherical coordinates. Let ρ_1 be the first Jacobi vector from He^{2+} to H^+, with reduced mass μ_1 and ρ_2 the second Jacobi vector from the center of mass of He^{2+} and H^+ to the electron, with reduced mass μ_2. The hyperradius R and hyperangle ϕ are defined as

$$R=\sqrt{\frac{\mu_1}{\mu}\rho_1^2+\frac{\mu_2}{\mu}\rho_2^2}, \tag{1}$$

$$\tan\phi=\sqrt{\frac{\mu_2}{\mu_1}}\frac{\rho_2}{\rho_1}, \tag{2}$$

where μ is arbitrary. In this paper we choose μ equal to the reduced mass μ_1 between the two nuclei. The hyperradius is then very close to the internuclear distance. We further define an angle θ as the angle between the two Jacobi vectors. By introducing the rescaled wave function $\Psi=\psi R^{3/2}\sin\phi\cos\phi$, we solve the Schrödinger equation in the form

$$\left(-\frac{1}{2}\frac{\partial}{\partial R}R^2\frac{\partial}{\partial R}+\frac{15}{8}+H_{ad}(R,\Omega,\hat{\omega})-\mu R^2E\right)\Psi(R,\Omega,\hat{\omega})=0, \tag{3}$$

where $\Omega\equiv\{\phi,\theta\}$, and $\hat{\omega}$ denotes the three Euler angles of the body-fixed frame axes with respect to the space-fixed frame. The H_{ad} is the adiabatic Hamiltonian with the hyperradius fixed:

$$H_{ad}(R,\Omega,\hat{\omega}) = \frac{\Lambda^2}{2} + \mu R^2 C(R,\Omega), \tag{4}$$

where Λ^2 is the square of the grand-angular momentum operator and $C(R,\Omega)$ is the total Coulomb interaction energy among the three particles [29]. The HSCC method treats the hyperradius R as a slow variable in the same way the BO approximation treats the internuclear distance. Thus we first solve the adiabatic equation to obtain adiabatic channel functions $\Phi^A_{\nu I}(R;\Omega)$. Here ν is the channel index, and I is the absolute value of the projection of total angular momentum $\boldsymbol{J}$ along the body-fixed z' axis, taken to be the axis between the two heavy particles. The superscript A designates the channel functions as adiabatic. We solve this equation by using B-spline basis functions. In the next step, similar to the standard BO approach, we solve Eq. (3) by expanding the rescaled wave function on the adiabatic basis:

$$\Psi(R,\Omega,\hat{\omega}) = \sum_{\nu}\sum_{I} F_{\nu I}(R)\Phi^A_{\nu I}(R;\Omega)\tilde{D}^J_{IM_J}(\hat{\omega}). \tag{5}$$

In this equation, $\tilde{D}$ is the normalized and symmetrized rotation function, and M_J is the projection of angular momentum $\boldsymbol{J}$ along the space-fixed z axis. The hyperradial wave functions satisfy the coupled equations

$$\left(-\frac{1}{2}\frac{\partial}{\partial R}R^2\frac{\partial}{\partial R} + \frac{15}{8} + U_{\lambda I} - \mu R^2 E\right)F_{\lambda I}(R) - \frac{R^2}{2}\sum_{\nu I'}(W_{\lambda I,\nu I'}\delta_{II'} + V_{\lambda I,\nu I'})F_{\nu I'}(R) = 0, \tag{6}$$

where U is the adiabatic potential and V is the rotational coupling. The nonadiabatic couplings W are given by

$$W_{\lambda I,\nu I'}(R) = 2\left\langle \Phi^A_{\lambda I}\left|\frac{d}{dR}\right|\Phi^A_{\nu I'}\right\rangle\frac{d}{dR} + \left\langle \Phi^A_{\lambda I}\left|\frac{d^2}{dR^2}\right|\Phi^A_{\nu I'}\right\rangle, \tag{7}$$

where the angular brackets imply integration over the angular coordinates Ω. Note that the first term in this equation corresponds to the radial coupling. These radial couplings can be computed accurately in the avoided crossing region only if adiabatic functions are calculated over very densely distributed meshed points. In the HSCC method as presented in [29], we solved the coupled hyperradial equations using R-matrix propagation [44] combined with the slow-smooth variable discretization (SVD) technique [45]. This method bypasses the tedious calculations of nonadiabatic couplings explicitly and the radial couplings are implicitly included in the overlaps between the channel functions at different hyperradii. In order to compare with the CRC method in detail for the present paper, approximate radial couplings have been extracted from the overlap matrix elements (see next section).

To compare the results from the HSCC method with the CRC method, there is, however, another complication. In the CRC approach, the adiabatic BO Hamiltonian for the present system is separable in spheroidal coordinates. This leads to real crossings of some of the adiabatic potential curves. In the HSCC method, the adiabatic Hamiltonian is not separable; thus, the adiabatic potential curves do not cross. Therefore, even if the same number of adiabatic channels are used in the calculation, the two approaches do not include the same channels in general. To be able to include exactly the same channels in the calculations, in practice we perform a "partial" diabatization procedure; that is, we diabatize only the needed sharp avoided crossings.

The adiabatic and diabatic representations are related by the unitary transformation

$$\Phi^D = C\Phi^A. \tag{8}$$

Here diabatic channel functions are denoted with a superscript D, and C is a unitary matrix. The transformation matrix C is chosen as the solution of the linear equation [46]

$$\frac{dC}{dR} - CP = 0, \tag{9}$$

where P is the radial coupling (for simplicity, we omit the I index in the following equations):

$$P_{\lambda\nu} = \left\langle \Phi^A_{\lambda}\left|\frac{d}{dR}\right|\Phi^A_{\nu}\right\rangle. \tag{10}$$

As mentioned above, in the HSCC method we adopt the SVD technique of Tolstikhin *et al.* [45] where nonadiabatic couplings (7) or radial couplings P, in particular, are implicitly included in the overlaps between the channel functions. Within the same spirit, we perform diabatization using only the overlap matrix elements. Specifically, we choose to approximate the derivative with respect to hyperradius R in Eqs. (9) and (10) by the simple difference

$$P_{\lambda\nu}(R) \approx \frac{1}{\Delta R}[\langle\Phi^A_{\lambda}(R)|\Phi^A_{\nu}(R+\Delta R)\rangle - \langle\Phi^A_{\lambda}(R)|\Phi^A_{\nu}(R)\rangle]. \tag{11}$$

Similarly, we have

$$\frac{dC_{\lambda\nu}}{dR} \approx \frac{1}{\Delta R}[C_{\lambda\nu}(R+\Delta R) - C_{\lambda\nu}(R)]. \tag{12}$$

Equation (9) then becomes

$$C_{\lambda\nu}(R+\Delta R) \approx \sum_{\mu} C_{\lambda\mu}(R)\langle\Phi^A_{\mu}(R)|\Phi^A_{\nu}(R+\Delta R)\rangle. \tag{13}$$

Thus the transformation matrix C can be obtained through the overlap matrix elements and the initial C. In practice, in order to diabatize the sharp avoided crossings we limit the summation in Eq. (13) to a few channels which have the largest overlaps. The diabatization should be started from a large enough distance where one can choose the initial condition for C to be the identity matrix. Once the diabatic basis is obtained, further implementation of the diabatic HSCC approach is straightforward with the adiabatic channel functions in the expansion (5) replaced by the diabatic ones.

A more detailed account of this diabatization procedure within the HSCC approach is given in Hesse *et al.* [47], where it is also used to eliminate channels that couple

weakly with the dominant channels, such that the number of basis functions in the coupled-channel calculations can be reduced.

B. Common-reaction-coordinate method

The CRC method is based on the use of the close-coupling expansion

$$\Psi^J(\boldsymbol{\rho}_2,\boldsymbol{\xi}) = \sum_k \chi_k(\boldsymbol{\xi})\Phi_k(\boldsymbol{\rho}_2;\xi), \tag{14}$$

where $\boldsymbol{\rho}_2$, as in Eq. (1), denotes the electronic position vector with respect to the center of mass of the two nuclei, the Φ_k are adiabatic BO wave functions, and the vector $\boldsymbol{\xi}$ is the common reaction coordinate. The CRC itself is a function of electronic and nuclear coordinates; it was introduced to ensure that the expansion (14) fulfills the scattering boundary conditions. In the application of the method, the molecular orbitals $\Phi_k(\boldsymbol{\rho}_2;\rho_1)$ are obtained by solving the BO electronic equation [48], and these orbitals are then evaluated at a point where ρ_1 (the internuclear separation) is numerically equal to ξ. It is easily noted that expansion (14) is identical to Eq. (5) when the reaction coordinate is defined by Eqs. (1) and (2). In our implementation, which is explained in detail in Ref. [17], the reaction coordinate is written as

$$\boldsymbol{\xi} = \boldsymbol{\rho_1} + \frac{1}{\mu}\boldsymbol{s}(\boldsymbol{\rho_1},\boldsymbol{\rho_2}) = \boldsymbol{\rho_1} + \frac{1}{\mu}\left[f(\rho_1,\rho_2)\boldsymbol{\rho_2} - \frac{1}{2}f^2(\rho_2,\rho_1)\boldsymbol{\rho_1}\right], \tag{15}$$

where $f(\rho_1,\rho_2)$ is a switching function that fulfills

$$\lim_{\rho_1\to\infty, r_A, \text{finite}} f(\rho_1,\rho_2) = -p,$$

$$\lim_{\rho_1\to\infty, r_B, \text{finite}} f(\rho_1,\rho_2) = q, \tag{16}$$

where r_A and r_B are the distances from the electron to nuclei A and B, respectively; $p\rho_1$ and $q\rho_1$ are the distances from the nuclear center of mass to nuclei A and B, respectively. With this definition, Ψ^J is a solution of the Schrödinger equation to $\mathcal{O}(\mu^{-1})$, in the limit of large internuclear separations. Substitution of Eq. (14) into the Schrödinger equation yields the system of differential equations

$$[(2\mu^{-1})\nabla_\xi^2 + (E-\epsilon_j)]\chi_j^J + \sum_k [2\mu^{-1}M_{jk}\cdot\boldsymbol{\nabla}_\xi + \langle\Phi_j|\nabla_\xi^2|\Phi_k\rangle] = 0, \tag{17}$$

where, as in all applications of the method, terms proportional to v^2 have been neglected, where $v = k_i/\mu$ and k_i is the initial momentum. The modified dynamical coupling M_{jk} is a vector whose component q has the form

$$M_{jk}^q = \left\langle \Phi_j \left| \frac{\partial}{\partial \xi_q} \right| \Phi_k \right\rangle + \langle\Phi_j|\boldsymbol{\nabla}(s_q)\cdot\boldsymbol{\nabla} + \nabla^2(s_q)|\Phi_k\rangle, \tag{18}$$

where ∇ denotes the gradient with respect to the electronic coordinate ρ_2.

In this work we have employed a CRC defined in terms of the switching function f of Harel and Jouin [48]:

$$f(\rho_1,\rho_2) = \frac{1}{2}[g_\alpha(\eta) + 1 - 2p], \tag{19}$$

with

$$g_\alpha = \alpha^{\alpha/2}\frac{\eta}{(\alpha - 1 + \eta^2)^{\alpha/2}} \tag{20}$$

and $\eta = \rho_1^{-1}(r_A - r_B)$. The parameter α was chosen to be 1.25 in the present calculation, but a test has been made to confirm that the results are insensitive to the values of α used (see [50] and references therein).

As shown in [17], using the eikonal approximation and assuming constant and state-independent nuclear velocity, one obtains the common translation factor (CTF) method as the high-energy limit of the CRC method, with the same switching function used to define the CRC and CTF; this CTF method describes asymptotically both the electronic radial motion and the rotation of the electronic cloud. In particular, the semiclassical limits of the present calculations are those reported in [51].

In practice, a transformation to diabatic basis is carried out, by using Eq. (9) with P equal to the radial component of the matrix $\boldsymbol{M}$, and the calculation of cross sections is evaluated by taking

$$\chi_k^J(\boldsymbol{\xi}) = \frac{1}{\xi}\mathcal{F}_{kl}^J\tilde{D}_{IM_J}^J(\hat{\omega}), \tag{21}$$

where we have employed the same notation as in Eq. (5). The ensuing set of radial equations is solved numerically and the elements of the scattering matrix S_{ij}^J are obtained from the numerical solution employing standard collision theory. The total cross section for transition from state i to state j is given by

$$\sigma_{ij} = \frac{\pi}{k_i^2}\sum_J \sigma_{ij}^J = \frac{\pi}{k_i^2}\sum_J (2J+1)|S_{ij}^J|^2. \tag{22}$$

C. Comparing HSCC and CRC formulations

The brief summary in the two previous subsections clearly demonstrated the similarity and difference in the HSCC and CRC methods. Formally the two methods appear to be equivalent if the hyperradius R is identified with the reaction coordinate ξ. Both methods are correct asymptotically to order $\mathcal{O}(\mu^{-1})$, a major improvement over the PSS approach. Comparing Eq. (15) with Eq. (1) where $\mu_1 = \mu$ and $\mu_2 = 1.0$, both the hyperradius R and the reaction coordinate yield corrections to the internuclear separation ρ_1 by amounts proportional to ρ_2/μ. In the HSCC method the radial and rotational couplings have the simple mathematical forms as in the PSS approach, but the BO wave functions in the PSS theory are replaced by the adiabatic hyperspherical channel functions. In practice, in the CRC method the wave functions and potential energies are the same as in the PSS approach, but the modified coupling matrix elements, as shown in Eq.

(18), have a few additional terms. Both the HSCC and CRC methods remove the spurious asymptotic radial couplings and the use of a vector to define the CRC removes the spurious, slowly decreasing rotational couplings (see [18]). Another difference is the asymptotic potential energies in the HSCC method takes into account of the masses of the heavy particles, but not in the usual implementations of the CRC method, where these corrections are neglected (see Ref. [17]). Thus the HSCC method can be easily applied to study charge transfer in collisions such as $D^+ + H$ at low energies [52], but this would be more difficult using the CRC method. On the other hand, the CRC method has been extended to many-electron collision systems, while generalization of the HSCC method to many-electron systems would be much more difficult. Formally, within a given number of adiabatic channel functions, no additional approximations are made in the HSCC method. For the CRC method, there is still freedom in the choice of switching functions even when the number of channels is fixed, but in calculations it has been shown that the results are insensitive to variations in the switching functions in general. In the next section numerical results from the two methods are used to illustrate the two methods.

III. RESULTS AND DISCUSSIONS

A. Low-energy comparison

For collision energies below 200 eV, the dominant reaction channels are charge transfer to $He^+(n=2)$ excited states. Thus, for both the HSCC and CRC methods, in the present calculation we include only four channels, one is the incident channel $H(1s)+He^{2+}$, and the other three are the main charge-transfer channels $He^+(n=2)+H^+$. These four adiabatic potential curves included in the HSCC calculation are plotted in Fig. 1. The potential curves are labeled in terms of the molecular orbitals. As mentioned in the previous section, we have diabatized the adiabatic hyperspherical potential curves which transform the two sharp avoided crossings at about $R=1.7$ a.u. and 3.6 a.u. into real crossings. The inset shows the close-up of these curves that have been diabatized. These potential curves are essentially identical to the four adiabatic curves from the CRC method (not shown). We conclude that we use the same four channels in both calculations for the whole range of hyperradius (or internuclear separation).

In Figs. 2 and 3 we compare, respectively, the radial and rotational coupling matrix elements from the two methods. As mentioned in the previous section, in the HSCC approach the radial couplings are calculated approximately using Eq. (11). The rotational couplings are calculated explicitly in the HSCC method (see [29,30]). We can see good agreement from the two methods for R larger than about 6.0 a.u. At smaller distances, the agreement becomes less satisfactory for all the radial couplings. The rotational couplings $2p\sigma$-$2p\pi$ also differ somewhat for $R<6$ a.u., whereas the other two rotational couplings from the two methods are in good agreement. Note that in both figures we do not distinguish the hyperradius from the internuclear separation or

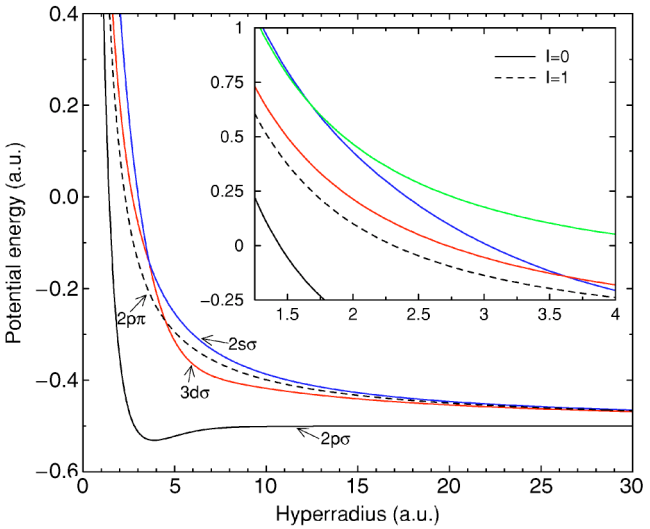

FIG. 1. (Color online) Potential curves included in the minimum four-channel HSCC calculations. The inset shows the close-up for the region near the two sharp avoided crossings at $R=1.7$ a.u. and 3.6 a.u. We have added the next upper channel in the inset to clearly illustrate the avoided crossing near 1.7 a.u.

from the reaction coordinates. They differ somewhat only for R much less than 1 a.u.

Figure 4 compares partial-wave charge-transfer cross sections at 200 eV. The agreement is very good for the whole range of partial waves J. We show on the inset for J from 150 up to 950 where the partial-wave cross sections are small. Here we also include the result from the DAO calculation of Fukuda and Ishihara [43]. The overall agreement among the three calculations are indeed quite impressive. We note that earlier calculations by Fukuda and Ishihara [43] and by Liu *et al.* [29] showed that, for the range of J indicated in the inset, the quantal results at this energy are very close to the semiclassical results by Winter and Hatton using MO's with plane-wave ETF [38].

The agreement between HSCC and CRC partial-wave cross sections is even better at 100 eV and 50 eV, shown in

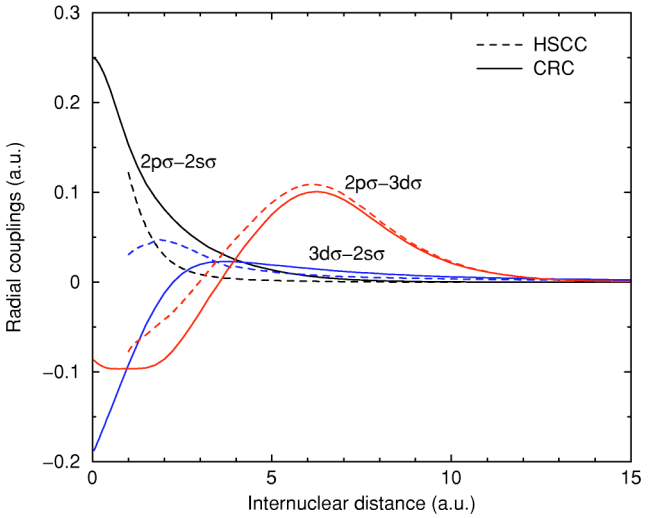

FIG. 2. (Color online) Comparison of radial couplings from the HSCC (dashed lines) and CRC (solid lines) methods.

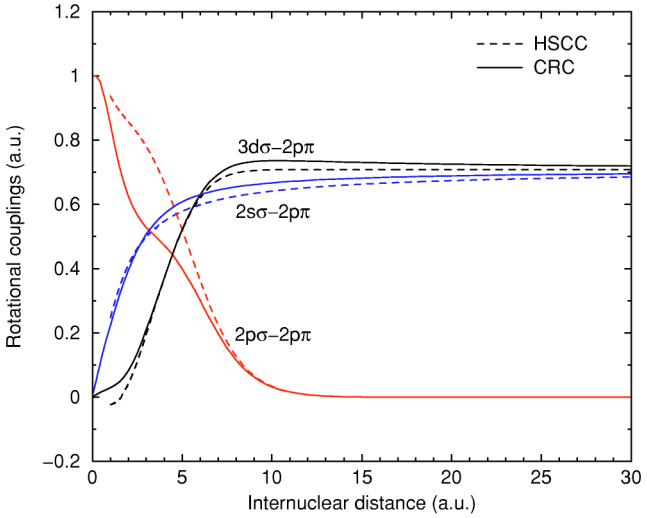

FIG. 3. (Color online) Comparison of rotational couplings from the HSCC (dashed lines) and CRC (solid lines) methods.

Figs. 5 and 6, respectively. The general behaviors of the cross sections at 200 eV and these two energies are very similar, with large contributions to the total cross section coming from relatively small partial waves J, below about $J=180$, 100, and 50, respectively. In fact, this general behavior remains the same for the whole range of energy from about 200 eV down to about 40 eV. In semiclassical language, the dominant transition occurs at impact parameters smaller than about 1.6 a.u. We noted that the prominent peaks at small J for this range of energy result mainly from rotational coupling, while the small peaks at larger J come mainly from radial couplings. This is in agreement with the results reported by Grozdanov and Solov'ev [41] and Janev *et al.* [42]. The good agreement of cross sections from the

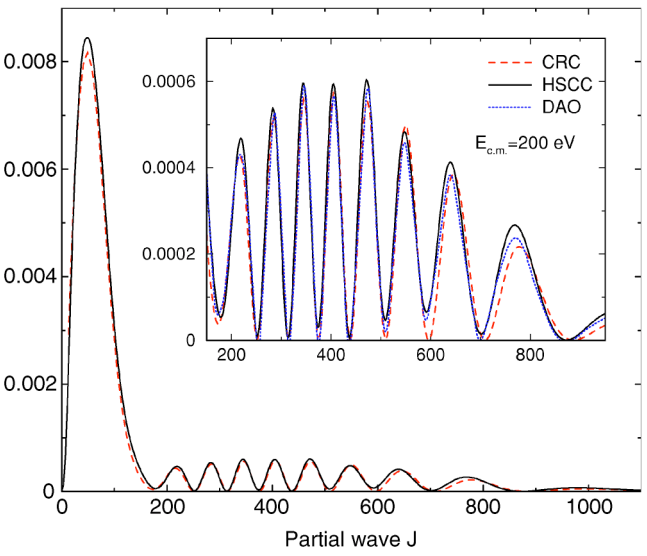

FIG. 4. (Color online) Comparison of partial-wave charge-transfer cross sections from the HSCC (solid line) and CRC (dashed line) methods at a collision energy of 200 eV. The inset shows the close-up for J from 150 up to 950. The results from the DAO method of Fukuda and Ishihara [43] are also shown (dotted lines).

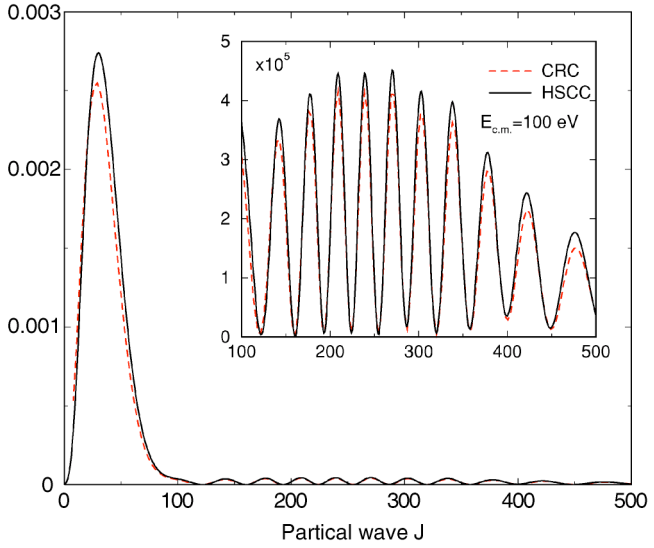

FIG. 5. (Color online) Comparison of partial-wave charge-transfer cross sections from the HSCC and CRC methods at a collision energy of 100 eV. The inset shows the good agreement for the higher J where the cross sections are very small.

two approaches indicates that differences in the radial and rotational couplings, as shown on Figs. 3 and 2, have only minor effects on the accuracy of the cross sections in this energy region.

The J-dependent behavior of the cross section is totally different at 30 eV, where the prominent peak at small J disappears; see Fig. 7. Still, the general behaviors remain similar in both approaches. The positions of the peaks are also in good agreement. However, the CRC cross section is noticeably smaller than that of the HSCC approach. It is interesting to note that at this energy the four-channel adiabatic HSCC calculation by Liu *et al.* [29] is very different from the present diabatic one for partial waves J smaller than about 50. For larger J the two results are identical. This indicates

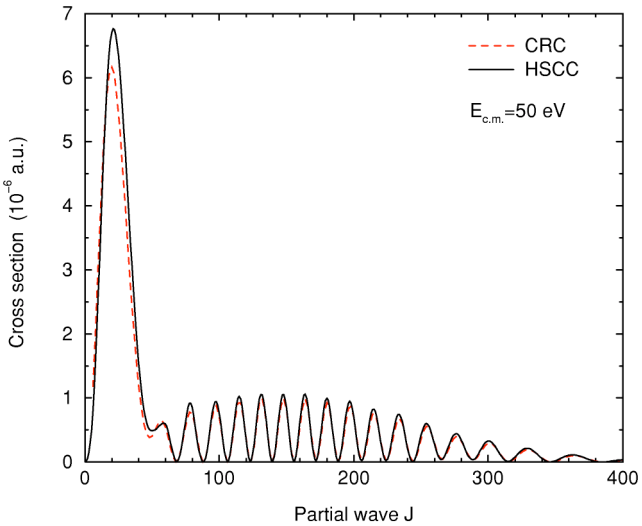

FIG. 6. (Color online) Comparison of the partial-wave charge-transfer cross sections from the HSCC and CRC methods at a collision energy of 50 eV.

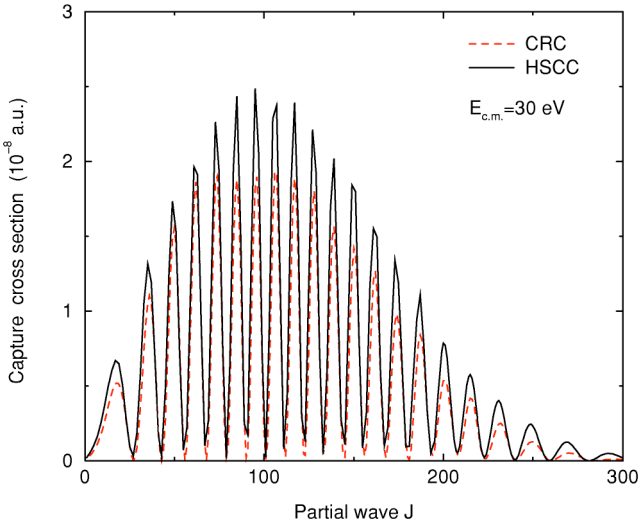

FIG. 7. (Color online) Comparison of the partial-wave charge-transfer cross section from the HSCC and CRC methods at a collision energy of 30 eV.

the importance of treating the avoided crossing near $R=1.7$ a.u. diabatically. In order to confirm this conjecture, we increased the number of channels included in both adiabatic and diabatic HSCC calculations. The results of diabatic HSCC calculations are stable with respect to the number of channels, whereas the adiabatic result converges to the diabatic one as more channels are included. This implies that the four-channel diabatic basis is better for describing the collision process at this energy. This is not surprising since this avoided crossing near $R=1.7$ a.u. is very sharp and narrow. In fact, in order to get converged results within the adiabatic HSCC approach, only the next upper channel needs to be included in the calculation (see the inset of Fig. 1).

At an even lower energy of 20 eV (see Fig. 8), the general behavior of the partial-wave cross section from the HSCC

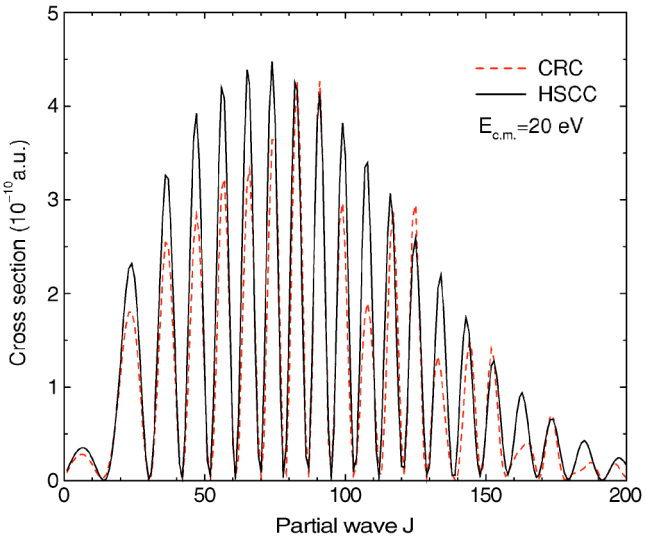

FIG. 8. (Color online) Comparison of the partial-wave charge-transfer cross section from the HSCC and CRC methods at a collision energy of 20 eV.

method is still similar to that of 30 eV, whereas the peaks from the CRC approach show some irregular oscillatory structure. As the cross section becomes very small, of the order of 10^{-10} a.u., the "spurious" structure might be an indication of the numerical instabilities in the CRC method or could be due to real differences between the two approaches at low energies. Note that similar differences have been observed in $Be^{4+}+H$ collisions [31] and $p+Na(3s)$ collisions at very low energies [30] previously.

At 20 and 30 eV, we have found that radial coupling is the main mechanism for charge transfer, while above 50–200 eV, rotational coupling also plays an important part. For a higher range of energy, this was noticed previously by Grozdanov and Solov'ev [41] and Janev *et al.* [42]. We have also checked the convergence of the charge-transfer cross sections from both calculations to confirm that adding more channels does not alter the results for energies below 200 eV.

B. Convergence of the HSCC and CRC calculations at higher energies

It is interesting to compare the results from the quantal approaches such as the HSCC and CRC methods in the higher-energy region, where one can compare them with the more widely available results from semiclassical calculations and experiments.

As the collision energy increases, the transition becomes less state selective and the minimum four-channel basis set shown in Fig. 1 would become less adequate. In this subsection we test the convergence of the two quantal methods at 600 eV and 1.6 keV and compare them with the semiclassical close-coupling approaches based on atomic orbitals (AO's) and on molecular orbitals including common translation factors. The two semiclassical methods have been extensively tested and employed for collisions in the higher-energy region.

In this higher-energy region we performed 20-channel and 10-channel HSCC calculations. We used diabatic basis functions and for the 20-channel calculations all the $I=0$ and $I=1$ channels that dissociate up to $He^+(n=4)$ are included, while for the 10-channel calculations they include all the channels up to $He^+(n=3)$.

To test the convergence of each quantal method, we compare the impact parameter weighted charge-transfer probabilities versus impact parameter. The partial-wave cross section is converted to the impact-parameter-dependent probability by

$$\sigma^J = \frac{2\pi b P(b)}{k}, \tag{23}$$

with $J=kb$, where k is the momentum. In Figs. 9(a) and 10(a) we show the results from HSCC at 600 eV and 1.6 keV, respectively. We also plot in these figures the results from the AO calculations using 14-state basis set [53]. Note that these AO results agree with the CTF results shown in Figs. 9(b) and 10(b) and, for all practical purposes, are also in agreement with the semiclassical MO results from Hatton *et al.* [37] and Winter and Hatton [38]. Thus we will treat these

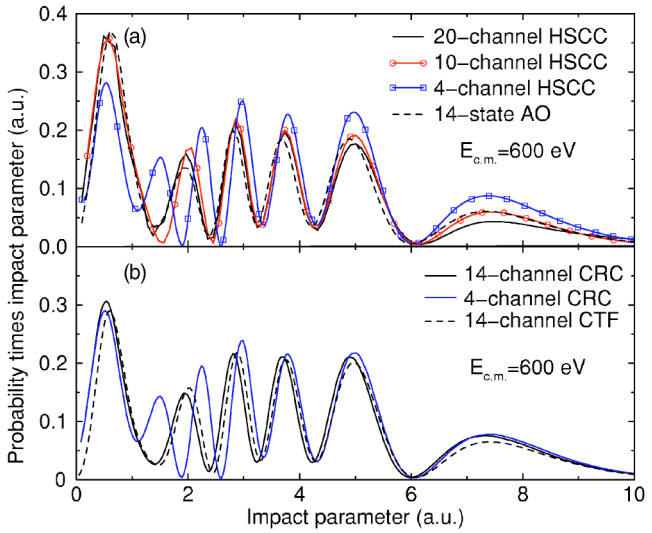

FIG. 9. (Color online) Convergence of the HSCC (a) and CRC (b) methods with respect to the number of channels included in calculations for the collision energy of 600 eV. These quantal results are compared to the semiclassical AO calculations and the semiclassical CTF calculations; see text.

semiclassical results as converged. At 600 eV, clearly the 4-channel calculation is not enough, but the 10- and 20-channel calculations appear to have converged already. At 1.6 keV, on the other hand, for both the 10- and 20-channel calculations, even though the oscillations are well reproduced, the magnitudes are off, especially at larger impact parameters. At both energies, clearly the 4-channel calculations overestimate the capture probabilities. This has been observed already in earlier work by Liu *et al.* (see Table II and Fig. 6 from [29]).

The convergence tests on the CRC method are shown in Figs. 9(b) and 10(b). At 600 eV, the 14-channel CRC cross sections agree perfectly with the same 14-channel semiclassical CTF results (or the AO results). The 4-channel CRC is adequate at large impact parameters but not at small impact parameters. For 1.6 keV, at large impact parameters the 4-channel and 14-channel CRC agree with each other, but they deviate from the 14-channel semiclassical CTF results. Again the 4-channel CRC is not adequate at small impact parameters.

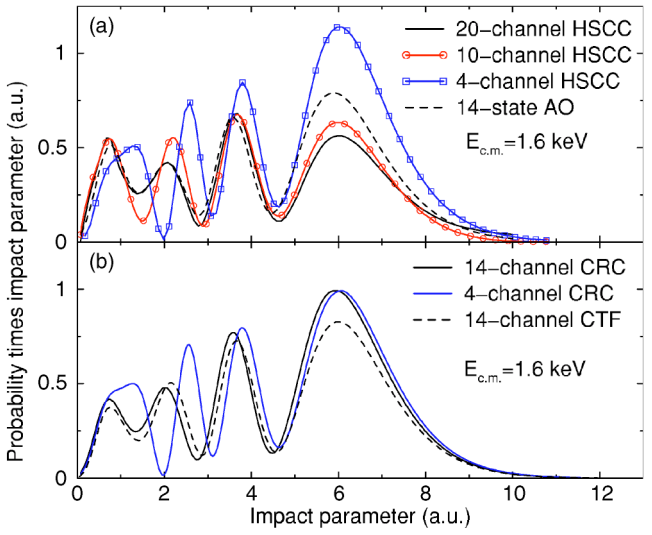

FIG. 10. (Color online) Convergence of the HSCC (a) and CRC (b) methods with respect to the number of channels included in calculations for the collision energy of 1600 eV. These quantal results are compared to the semiclassical AO calculations and the semiclassical CTF calculations; see text.

What can one conclude from these comparisons? The deficiency of the 4-channel calculations at small impact parameters can be easily attributed to the lack of enough channels at small impact parameters. In fact, the potential curves at small internuclear separations are quite close to each other and coupling to the higher channels becomes important as the collision energy increases. The agreement between the 4-channel and 14-channel CRC calculations at large impact parameters indicates that convergence with respect to the number of channels is not the issue. The fact that they agree with the CTF results at 600 eV but not at 1.6 keV is attributed to the approximation of neglecting v^2 terms in the CRC couplings, which are included in the semiclassical CTF calculation, leading to an overestimate of the charge-transfer probabilities, as shown in Figs. 9(b) and 10(b). To verify this, we performed a CTF calculation without the v^2 term and confirmed that the cross sections at large impact parameters are indeed very close to that of the CRC approach. For the HSCC method, the results in Figs. 9(a) and 10(a) illustrate the slow convergence of the method at increasing energies. In the HSCC method there are no equivalent factors like the switching functions or the electron translation factors to incorporate the translational effect of an electron moving with one or the other atomic center. Within the HSCC formulation, the only way that such a translational effect can be included is to increase the number of channels. The convergence in such calculations is expected to be very slow as the collision energy is increased. On the other hand, semiclassical methods for collisions in this energy regime are now well established, so there is no need to push the quantum collision theories to this higher-energy regime.

IV. SUMMARY AND CONCLUSIONS

In this paper, in the example of a simple collision system—namely, $He^{2+}+H$—we gave a detailed comparison of the HSCC and CRC methods at the level of partial-wave cross sections over a broad range of collision energy. We found very good agreement between the two methods at low energies from 30 eV up to 200 eV. Similar agreements at the total cross section levels have also been observed in two other systems previously [30,31]. Since the two methods are quite different computationally, this good agreement is a strong indication of the validity of both methods. We can therefore safely conclude that both methods are capable of obtaining accurate cross sections for collisions at low energies even if there is a lack of experimental data. This is of

practical importance since, while the HSCC method can be used so far only for one-electron ion-atom collision systems, the CRC approach has been applied to many-electron cases. One can expect that these calculations are reliable if the structure part of the CRC calculations are done correctly and accurately. We note, however, that the remaining discrepancies seen at energies below about 30 eV might indicate either numerical instabilities of the CRC method and/or sensitivity of the results to the form of reaction coordinates used in the calculations since similar discrepancies have been found for weaker channels in other collision systems [31,32]. In the higher-energy region where available results from the semiclassical calculations are quite satisfactory, we have shown that the quantal HSCC and CRC methods merge reasonably well with the semiclassical AO or CTF theories. Without any explicit factors to account for the translational effects, but rather by a modification of the internuclear variable, the HSCC method has been shown to converge slower than the other approaches at higher energies. On the other hand, theoretical approaches for ion-atom collisions at higher energies are well established and there is no need to extend the HSCC method to such a higher-energy region.

ACKNOWLEDGMENTS

This work was supported in part by the Chemical Sciences, Geosciences and Biosciences Division, Office of Basic Energy Sciences, Office of Science, U.S. Department of Energy, and by DGICYT (Spain) Project Nos. BFM2000-0025 and FTN2000-0911.

[1] B. H. Bransden and M. R. C. McDowell, *Charge Exchange and Theory of Ion-Atom Collisions* (Clarendon, Oxford, 1992).
[2] H. S. Massey and R. A. Smith, Proc. R. Soc. London, Ser. A **142**, 142 (1933).
[3] D. R. Bates and R. McCarroll, Proc. R. Soc. London, Ser. A **245**, 175 (1958).
[4] M. Kimura and N. F. Lane, Adv. At., Mol., Opt. Phys. **26**, 79 (1989).
[5] W. Fritsch and C. D. Lin, Phys. Rep. **202**, 1 (1991).
[6] S. B. Schneiderman and A. Russek, Phys. Rev. **181**, 311 (1969).
[7] L. F. Errea, C. Harel, H. Jouin, L. Méndez, B. Pons, and A. Riera, J. Phys. B **27**, 3603 (1994).
[8] E. A. Solov'ev, in *Proceedings of the XIX ICPEAC* (Whistler, Canada), edited by L. J. Dube *et al.* (AIP Press, New York, 1995), p. 471.
[9] E. A. Solov'ev, Sov. Phys. Usp. **32**, 228 (1989).
[10] M. C. van Hemert, E. F. van Dishoeck, I. A. van der Hart, and F. Koike, Phys. Rev. A **31**, 2227 (1985).
[11] N. Shimakura and M. Kimura, Phys. Rev. A **44**, 1659 (1991).
[12] M. H. Mittleman, Phys. Rev. **188**, 221 (1969).
[13] W. R. Thorson and J. B. Delos, Phys. Rev. A **18**, 135 (1978).
[14] J. B. Delos, Rev. Mod. Phys. **53**, 287 (1981).
[15] M. Gargaud, R. McCarroll, and P. Valiron, J. Phys. B **20**, 1555 (1987).
[16] H. Croft and A. S. Dickinson, J. Phys. B **29**, 57 (1996).
[17] L. F. Errea, C. Harel, H. Jouin, L. Méndez, B. Pons, and A. Riera, J. Phys. B **31**, 3527 (1998).
[18] R. McCarroll and D. S. F. Crothers, Adv. At., Mol., Opt. Phys. **32**, 253 (1994).
[19] A. Riera, Mol. Phys. **88**, 199 (1996).
[20] T. Mroczkowski, D. Savin, R. Rejoub, P. S. Krstic, and C. C. Havener, Phys. Rev. A **68**, 032721 (2003), and references therein.
[21] C. D. Lin, Phys. Rep. **257**, 1 (1995).
[22] B. LePetit and J. M. Launay, Chem. Phys. Lett. **151**, 287 (1988).
[23] D. Skouteris, J. F. Castillo, and D. E. Manolopoulos, Comput. Phys. Commun. **133**, 128 (2000).
[24] J. Z. Tang, S. Watanabe, M. Matsuzawa, and C. D. Lin, Phys. Rev. Lett. **69**, 1633 (1992).
[25] D. Kato and S. Watanabe, Phys. Rev. A **56**, 3687 (1997).
[26] Y. Zhou and C. D. Lin, J. Phys. B **27**, 5065 (1994).
[27] A. Igarashi, I. Shimamura, and N. Toshima, Phys. Rev. A **58**, 1166 (1998).
[28] B. D. Esry, C. H. Greene, and J. P. Burke, Jr., Phys. Rev. Lett. **83**, 1751 (1999).
[29] C. N. Liu, A. T. Le, T. Morishita, B. D. Esry, and C. D. Lin, Phys. Rev. A **67**, 052705 (2003).
[30] A. T. Le, C. N. Liu, and C. D. Lin, Phys. Rev. A **68**, 012705 (2003).
[31] A. T. Le, M. Hesse, T. G. Lee, and C. D. Lin, J. Phys. B **36**, 3281 (2003).
[32] T. G. Lee, A. T. Le, and C. D. Lin, J. Phys. B **36**, 4081 (2003).
[33] C. N. Liu, A. T. Le, and C. D. Lin, Phys. Rev. A **68**, 062702 (2003).
[34] B. Herrero, I. L. Cooper, A. S. Dickinson, and D. R. Flower, J. Phys. B **28**, 711 (1995).
[35] J. F. Castillo and L. Méndez, Phys. Rev. A **56**, 421 (1997).
[36] R. D. Piacentini and A. Salin, J. Phys. B **13**, 1666 (1974).
[37] G. J. Hatton, N. F. Lane, and T. G. Winter, J. Phys. B **12**, L571 (1979).
[38] T. G. Winter and G. J. Hatton, Phys. Rev. A **21**, 793 (1980).
[39] M. Kimura and W. R. Thorson, Phys. Rev. A **24**, 3019 (1981).
[40] L. F. Errea, J. M. GomezLlorente, L. Méndez, and A. Riera, Phys. Rev. A **32**, 2158 (1985).
[41] T. P. Grozdanov and E. A. Solov'ev, Phys. Rev. A **42**, 2703 (1990).
[42] R. K. Janev, J. Pop-Jordanov, and E. A. Solov'ev, J. Phys. B **30**, L353 (1997).
[43] H. Fukuda and T. Ishihara, Phys. Rev. A **46**, 5531 (1994).
[44] J. C. Light and R. B. Walker, J. Chem. Phys. **66**, 4272 (1976).
[45] O. I. Tolstikhin, S. Watanabe, and M. Matsuzawa, J. Phys. B **29**, L389 (1996).
[46] F. T. Smith, Phys. Rev. **179**, 111 (1969).
[47] M. Hesse, A. T. Le, and C. D. Lin, Phys. Rev. A **69**, 052712 (2004).

[48] J. D. Power, Philos. Trans. R. Soc. London, Ser. A **274**, 663 (1973).
[49] C. Harel and H. Jouin, Europhys. Lett. **11**, 2121 (1990).
[50] L. F. Errea, C. Harel, C. Illescas, H. Jouin, L. Méndez, B. Pons, and A. Riera, J. Phys. B **31**, 3199 (1998).
[51] C. Harel, H. Jouin, and B. Pons, At. Data Nucl. Data Tables **68**, 279 (1998).
[52] A. Igarashi and C. D. Lin, Phys. Rev. Lett. **83**, 4041 (1999).
[53] J. Kuang and C. D. Lin, J. Phys. B **30**, 101 (1997).